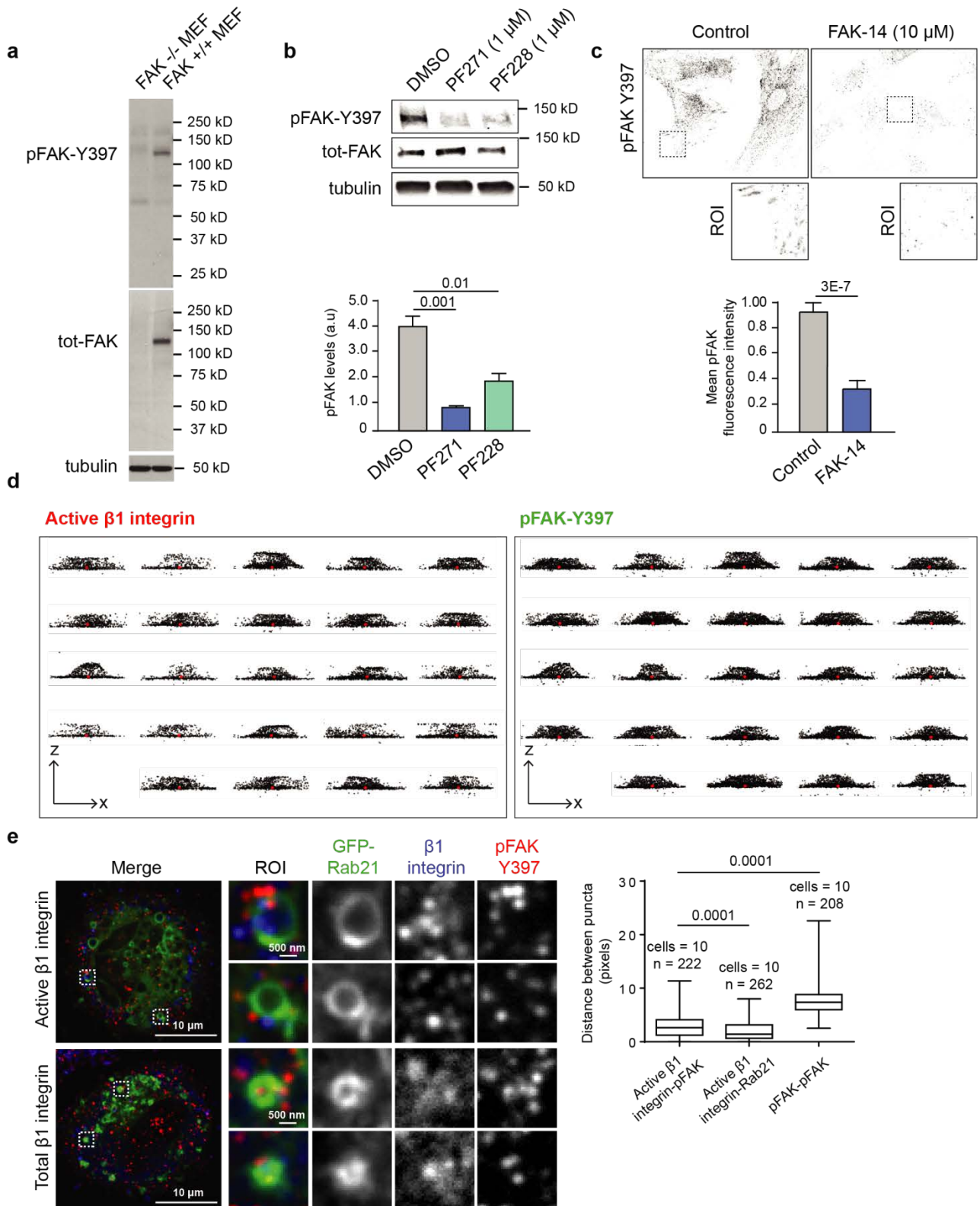


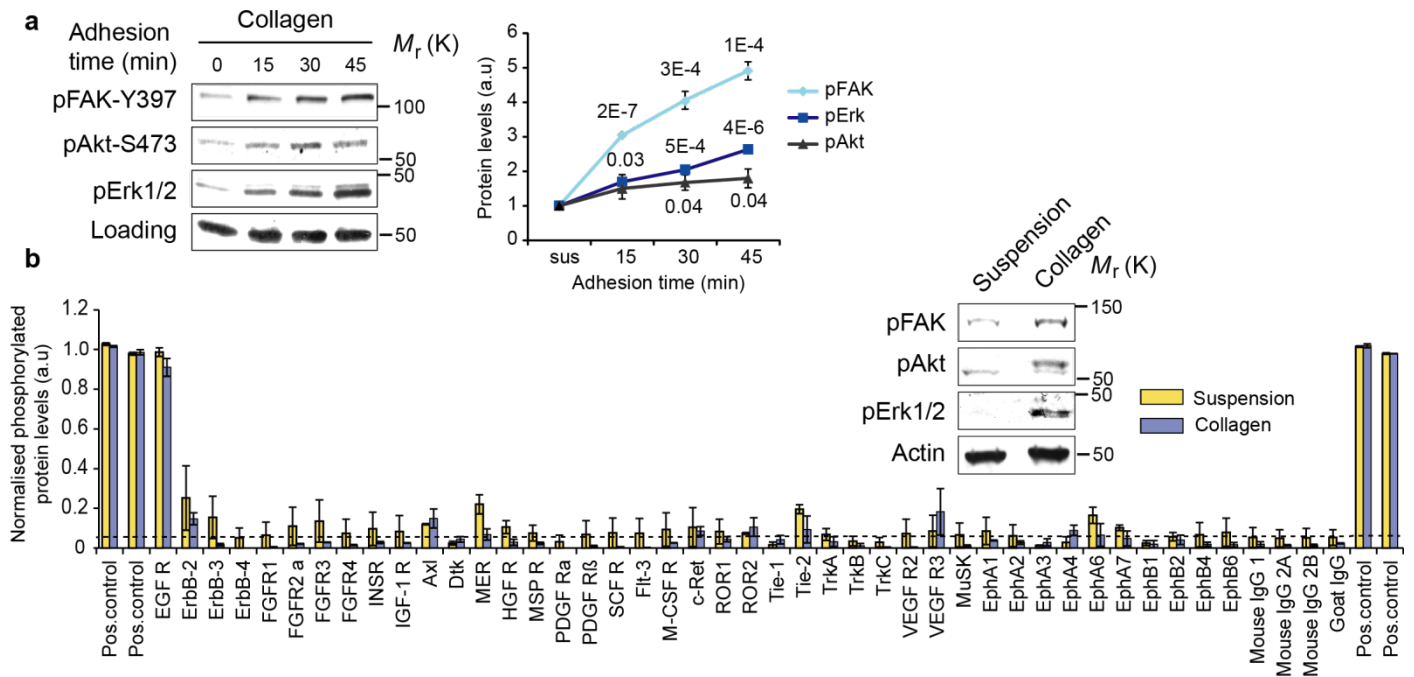
Alanko et al., 2015. Integrin Endosomal Signalling Suppresses Anoikis

- Supplementary figures
- Supplementary figure legends
- Table legends

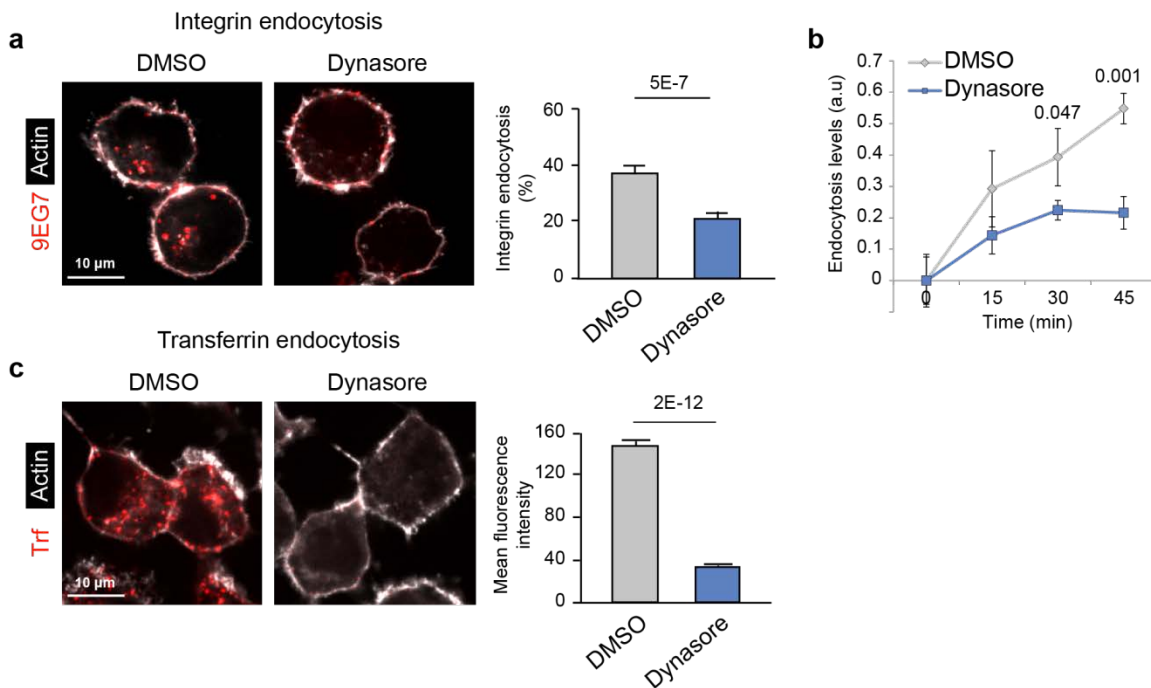


Supplementary Figure 1. Validation of the pFAK-Y397 antibody. **a, b** Validation of the pFAK-Y397 antibody in FAK^{-/-} and FAK^{+/+} MEF cell lysates (**a**) and in TIFFs in the presence of FAK-Y397 phosphorylation inhibitors (1 μ M PF271 or PF228) (**b**) (mean \pm SEM, n = 3 independent experiments). Statistics source data can be found in Supplementary Table 2. **c**, Quantification of pFAK-Y397 levels following FAK-14 inhibitor (10 μ M) treatment. Representative confocal images and ROIs of focal adhesions are shown (mean fluorescence intensity \pm SEM, n = 22 cells pooled from two independent experiments). **d**, Individual fluorescence density plots of MDA-MB-231 cells plated on crossbow-shaped fibronectin-coated micropatterns and stained for active β 1-integrin and pFAK-Y397. Shown are x-axis views. The analysis of these cells was used to generate the 3D probabilistic density plots shown in Figure 1a. **e**, Confocal images of pFAK-Y397 and total or active β 1-integrin staining in GFP-Rab21 overexpressing TIFFs plated on fibronectin (45 min). Representative ROIs from endosomes and box plot of the distance between adjacent puncta of active β 1-integrin and pFAK or Rab21 in GFP-Rab21-positive endosomes or of pFAK and pFAK outside the endosomes (in pixels) (box plots show the 25th–75th percentiles delineated by the upper and lower limits of the box; the median is shown by the horizontal line inside the box. Whiskers indicate maxima and minima). n= the number of active β 1-integrin-pFAK, active β 1-integrin-Rab21 and pFAK-pFAK doublets (indicated in the figure) analysed from multiple cells (numbers indicated in the figure) from three independent experiments are indicated.

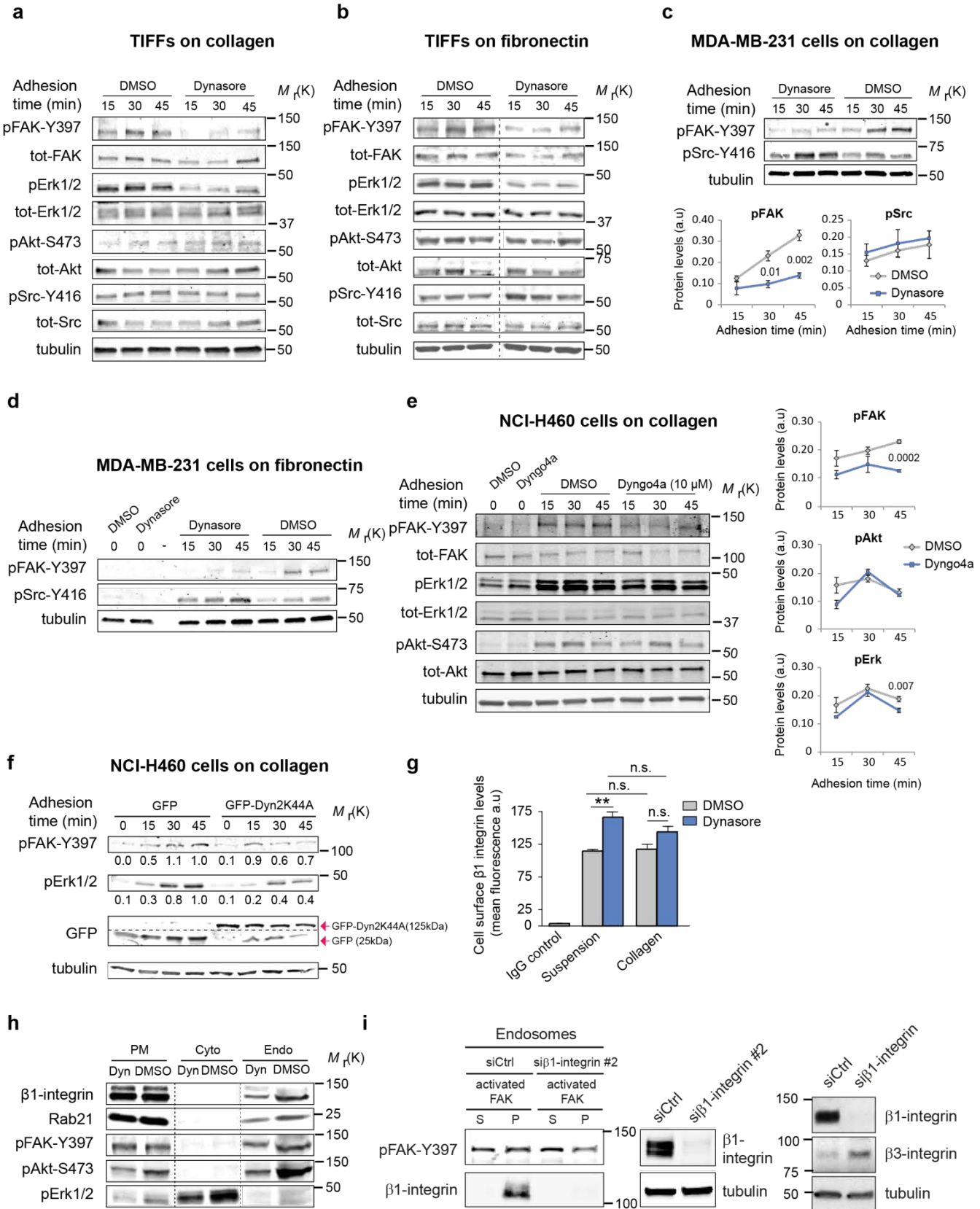
Mann-Whitney test *P* values are provided.



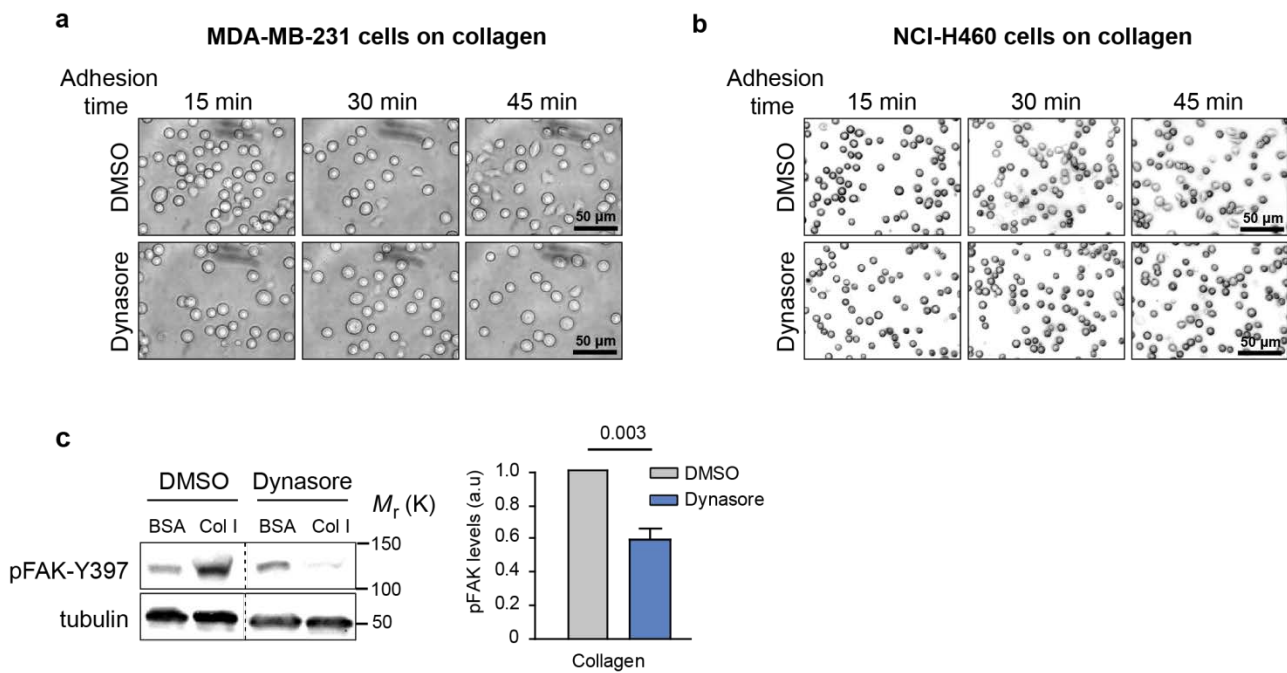
Supplementary Figure 2. ECM-induced downstream signalling is not due to growth factor receptor activation. **a**, Quantification of kinase activity in NCI-H460 cells plated on collagen. Representative blots are shown (mean \pm SEM, $n=3$ independent experiments). **b**, Quantification of human phospho-receptor tyrosine kinase array in NCI-H460 cells kept in suspension or plated on collagen (45 min). Positive control is an antibody against phospho-tyrosine. Representative blots of cell lysates used for the array are shown (mean phosphoprotein detection \pm SEM from two independent experiments). Student's two-tailed unpaired t -test P values are provided and statistics source data can be found in Supplementary Table 2. Uncropped images of blots are shown in supplementary figure 9.



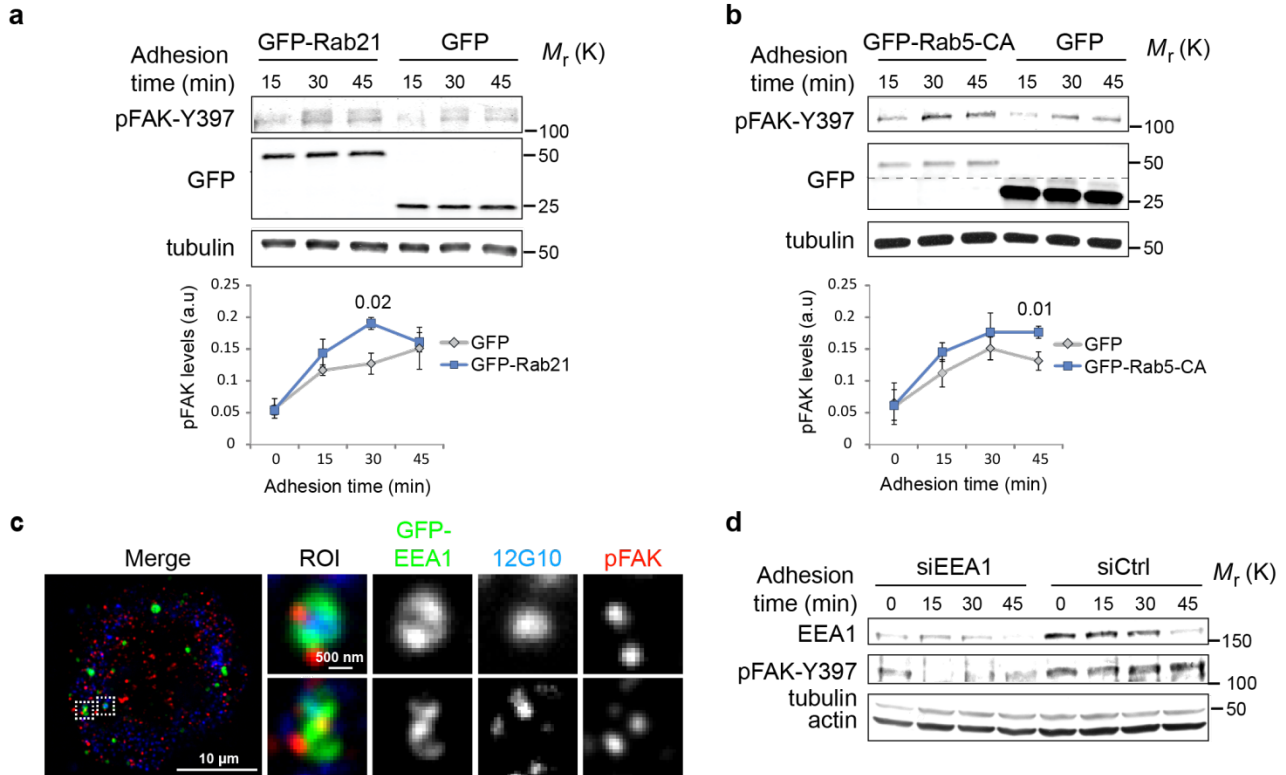
Supplementary Figure 3. Dynamin inhibition downregulates integrin receptor endocytosis. a, b Integrin receptor endocytosis in NCI-H460 cells plated on collagen for 45 min in the presence of active β 1-integrin (9EG7) antibody (45 min) \pm dynasore. **a**, Representative confocal images and quantification of the proportion of endocytosed integrin receptors based on antibody staining (n(DMSO)=52 cells, n(dynasore)=54 cells, pooled from three independent experiments, mean \pm SEM). **b**, Flow cytometry-based analysis of integrin endocytosis. Receptor internalisation, at the indicated time points, was calculated as an inverse ratio of total 9EG7-labelled integrin remaining on the cell surface compared to time point 0 (mean \pm SEM, n=3 independent experiments). **c**, Transferrin endocytosis in NCI-H460 cells plated on collagen for 45 min in the presence of 555-labelled-transferrin (15 min) \pm dynasore. Representative confocal images and quantification of the total levels of endocytosed transferrin are shown (n(DMSO)=35 cells, n(dynasore)=32 cells, pooled from three independent experiments, mean \pm SEM). Student's two-tailed unpaired t-test *P* values are provided. Statistics source data can be found in Supplementary Table 2.



Supplementary Figure 4. Inhibition of integrin endocytosis attenuates integrin signalling. **a, b** Representative blots of kinase activity in TIFFs plated on collagen (**a**, quantified in Fig. 3c) and fibronectin (**b**, quantified in Fig. 3d) \pm dynasore. **c, d**, Analysis of kinase activity in MDA-MB-231 cells plated on collagen (**c**) and fibronectin (**d**) \pm dynasore. Representative blots (**c, d**) and quantification (**c**) are shown (mean \pm SEM, n=3 independent experiments). **e**, Analysis of kinase activity in NCI-H460 cells plated on collagen \pm 10 μ M Dyno4a. Representative blots and quantifications are shown (mean \pm SEM, n=3 independent experiments). **f**, Analysis of kinase activity in GFP or GFP-Dyn2K44A overexpressing NCI-H460 cells plated on collagen. Representative blot and quantification of normalised band integrated densities are shown (three independent experiments). **g**, Flow cytometry quantification of total cell surface β 1-integrin levels in NCI-H460 cells held in suspension or plated on collagen (45 min) \pm dynasore (mean fluorescence \pm SEM, n=3 independent experiments). **h**, Subcellular fractionation of NCI-H460 cells plated on collagen (45 min) \pm dynasore. Representative blots of the plasma membrane (PM), cytoplasm (Cyto) and endosomal fractions (Endo) are shown (three independent experiments). **i**, Representative immunoblot analysing the recruitment of recombinant FAK to purified endosomes derived from either control- or β 1-integrin-silenced FAK $-/-$ MEFs (different siRNA to one used in Fig. 4c; three independent experiments). Please note that silencing of β 1-integrin induces cellular levels of β 3-integrin. This might contribute to the residual FAK recruitment to the β 1-integrin silenced endosomal fraction. Student's two-tailed unpaired t-test *P* values are provided. Statistics source data can be found in Supplementary Table 2. Uncropped images of blots are shown in supplementary figure 9.

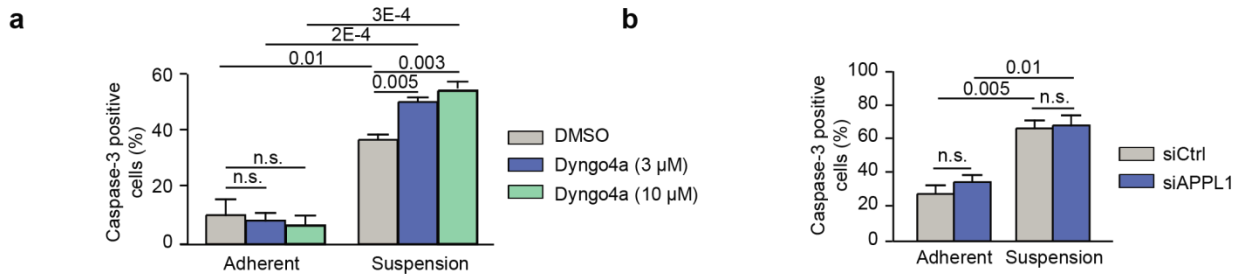


Supplementary Figure 5. Dynamin inhibition affects cell spreading. MDA-MB-231 cells (**a**) or NCI-H460 cells (**b**) plated on collagen for the indicated times \pm dynasore (three independent experiments). (**c**) Quantification of FAK activation (pFAK-Y397 levels) in NCI-H460 cells incubated with collagen (Col I) or BSA-coated beads in suspension (45 min) \pm dynasore (mean \pm SEM, $n=3$ independent experiments). Student's two-tailed unpaired t-test P values are provided and statistics source data can be found in Supplementary Table 2. Uncropped images of blots are shown in supplementary figure 9.



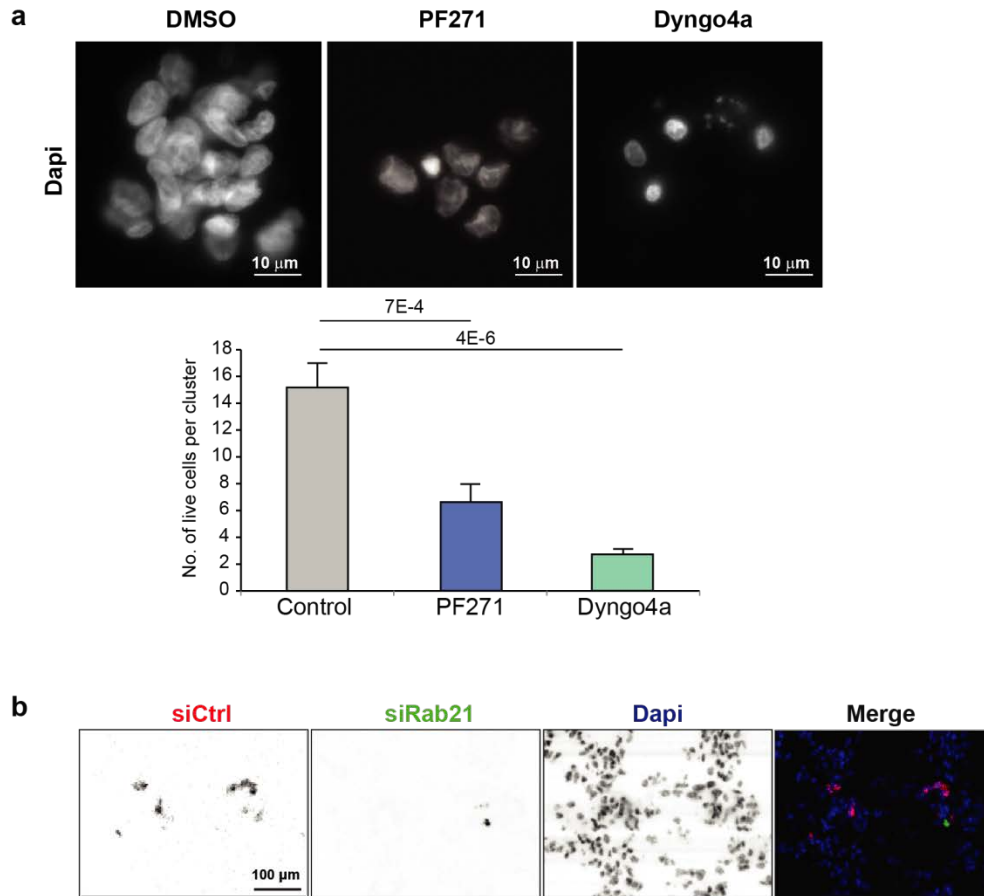
Supplementary Figure 6. Rab5, Rab21 and EEA1 are important for integrin-mediated FAK activation.

a, b, Representative blots and quantification of pFAK levels in GFP and GFP-Rab21 (**a**) or GFP-Rab5-CA (**b**) overexpressing MDA-MB-231 cells plated on collagen (n(a)=3, n(b)=6 independent experiments, mean \pm SEM). **c**, Active β 1-integrin (12G10) and pFAK-Y397 localization in GFP-EEA1 expressing TIFFs plated on fibronectin (45 min). **d**, Representative blot of pFAK-Y397 levels in control or EEA1 smart pool silenced NCI-H460 cells plated on collagen. Student's two-tailed unpaired t-test *P* values are provided and statistics source data can be found in Supplementary Table 2. Uncropped images of blots are shown in supplementary figure 9.



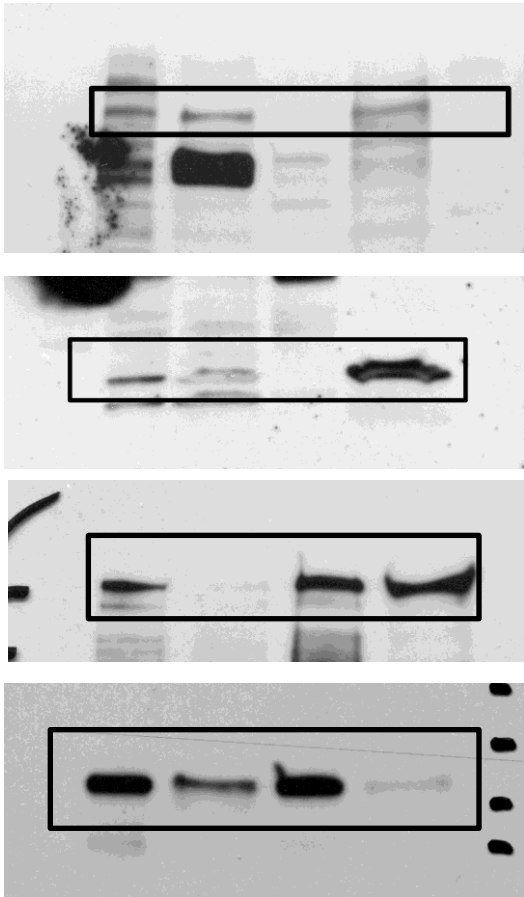
Supplementary Figure 7. APPL1 is not important for anoikis suppression.

a-b, Quantification of caspase-3 positive apoptotic TIFFs ± Dyngo4a (**a**), and following APPL1 silencing (**b**) (mean fluorescence ± SEM, n=3 independent experiments). Student's t-test *P* values are provided and statistics source data can be found in Supplementary Table 2.



Supplementary Figure 8. Anchorage-independent growth and metastases of MDA-MB-231 cells are sensitive to FAK and dynamin inhibition and Rab21 silencing. **a**, MDA-MB-231 cells were plated on agar and incubated with the indicated drugs. Anchorage-independent growth was assessed by counting the number of cells per cluster with intact nuclei (mean \pm SEM, $n = 6$ fields of view assessed from three independent experiments). **b**, Representative images showing extravasation of siCtrl- and siRab21-treated MDA-MB-231 cells in mouse lungs. Student's t-test P values are provided.

Figure 2.



Supplementary Figure 9. Uncropped Western blots

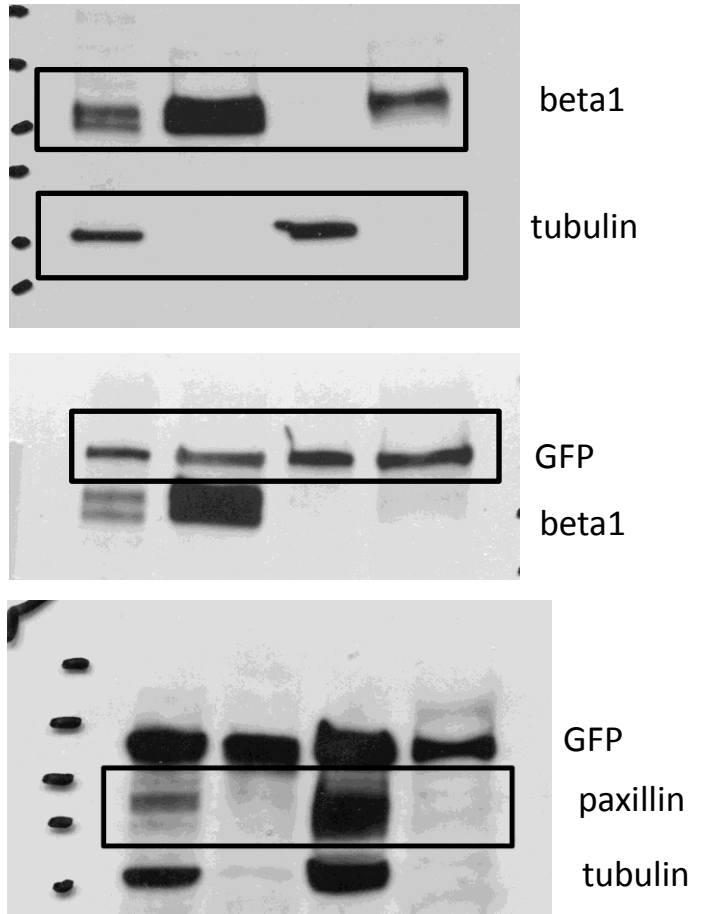
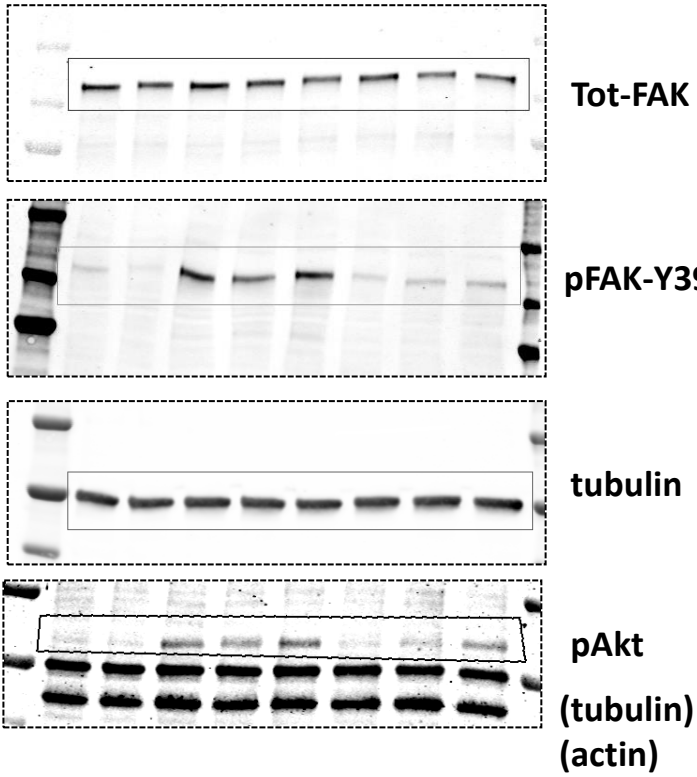


Figure 3a.



Supplementary Figure 9. Uncropped Western blots

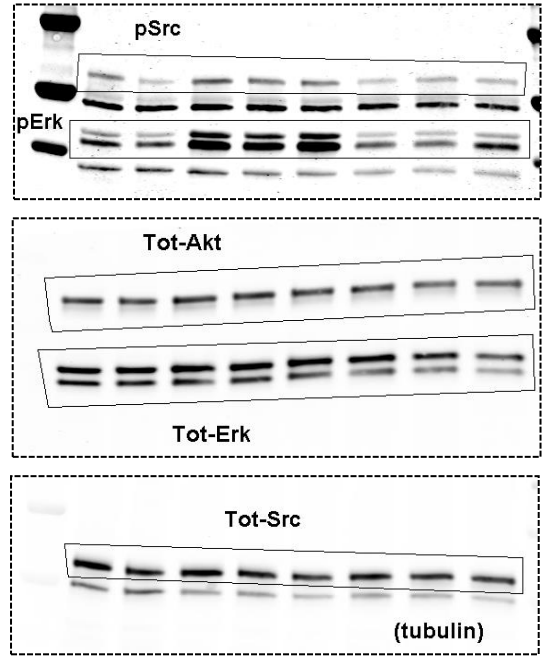


Figure 3b.

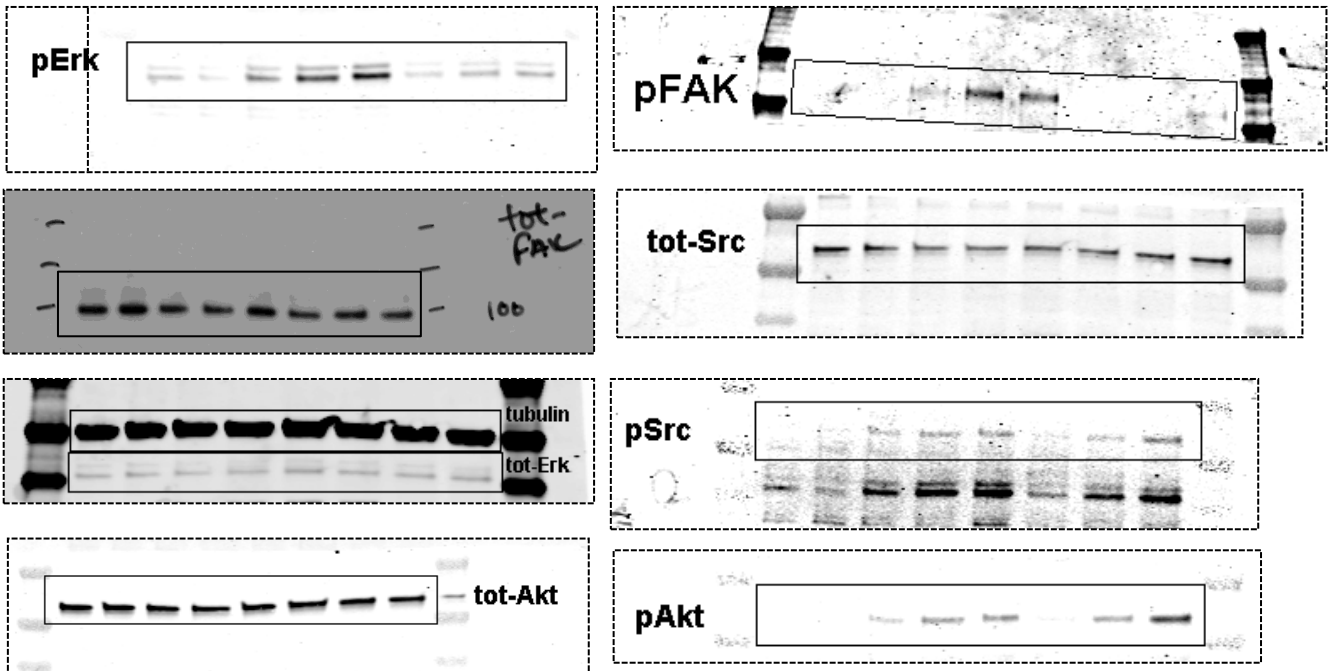


Figure 3f.

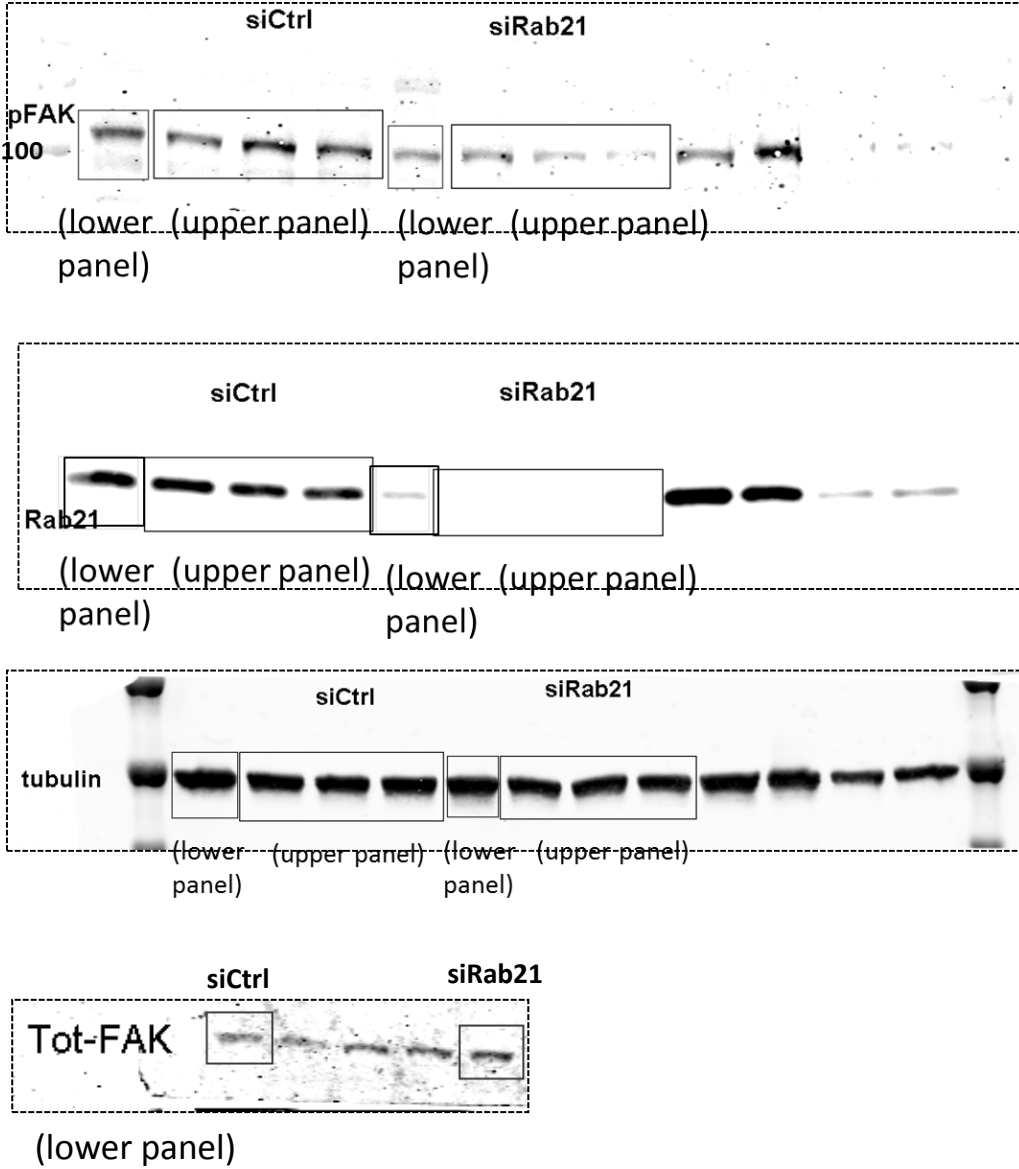


Figure 3g.

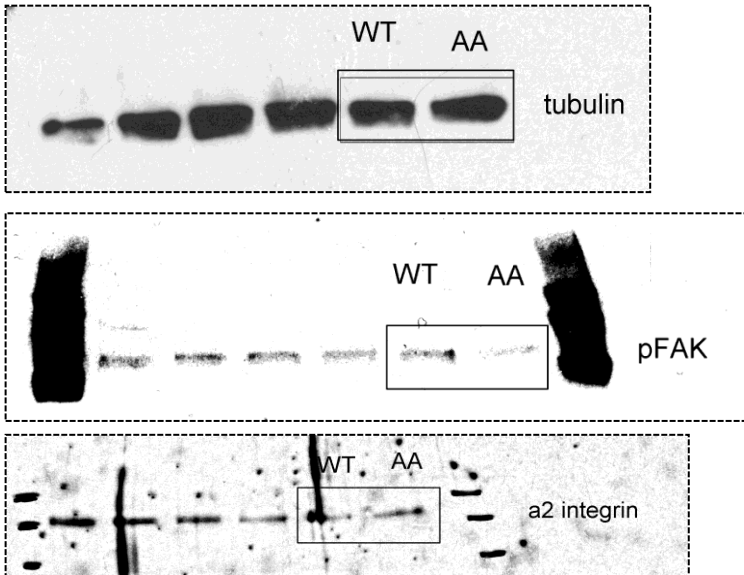


Figure 4a.

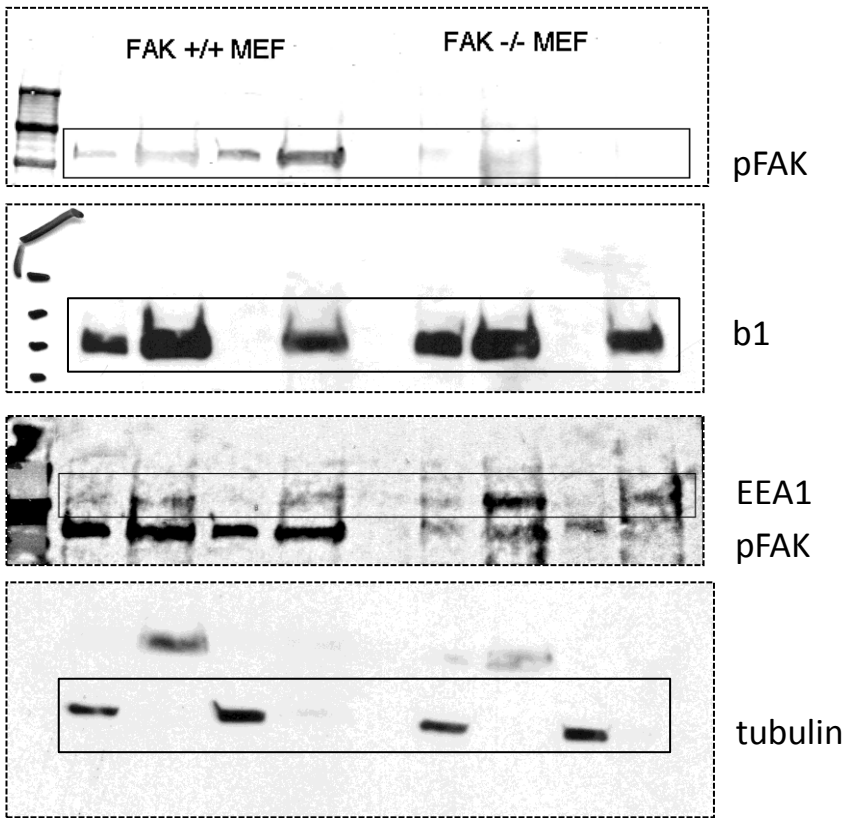


Figure 4b.

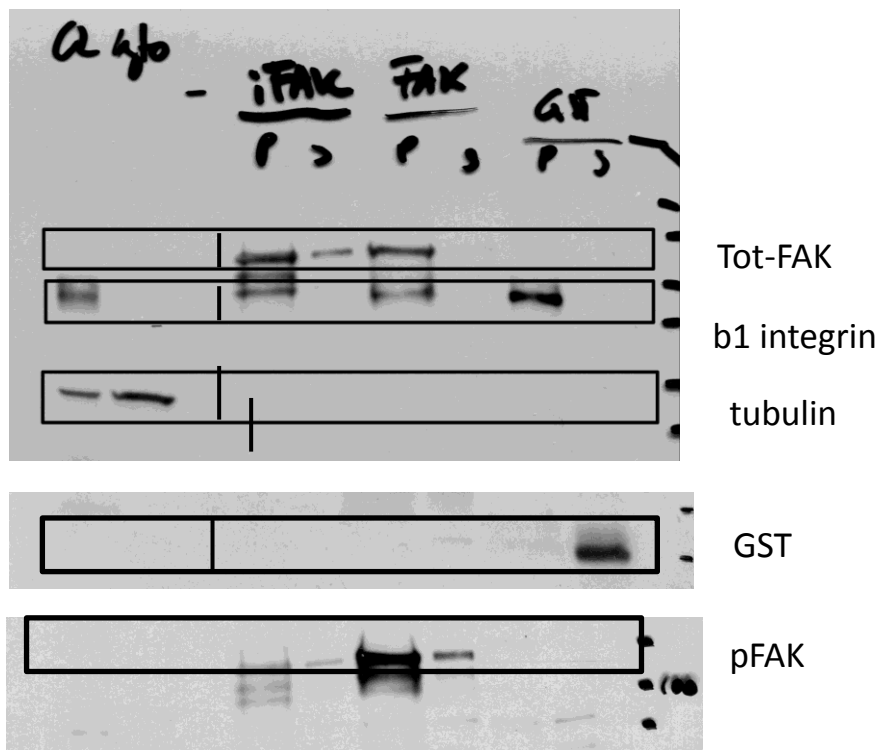
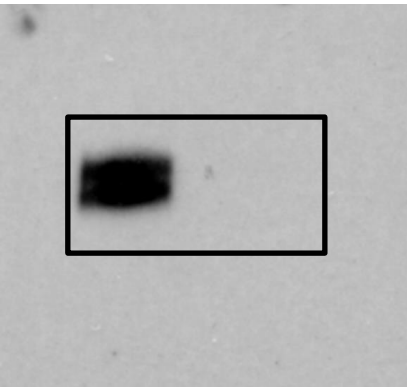
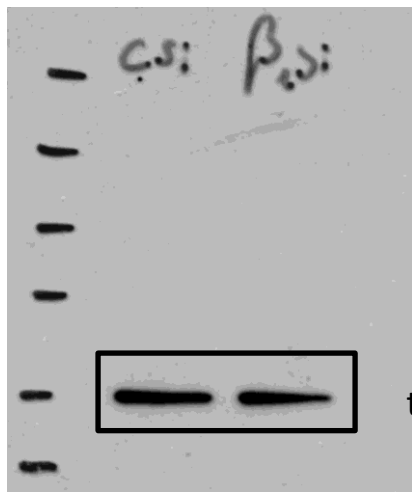


Figure 4c.



Supplementary Figure 9. Uncropped Western blots

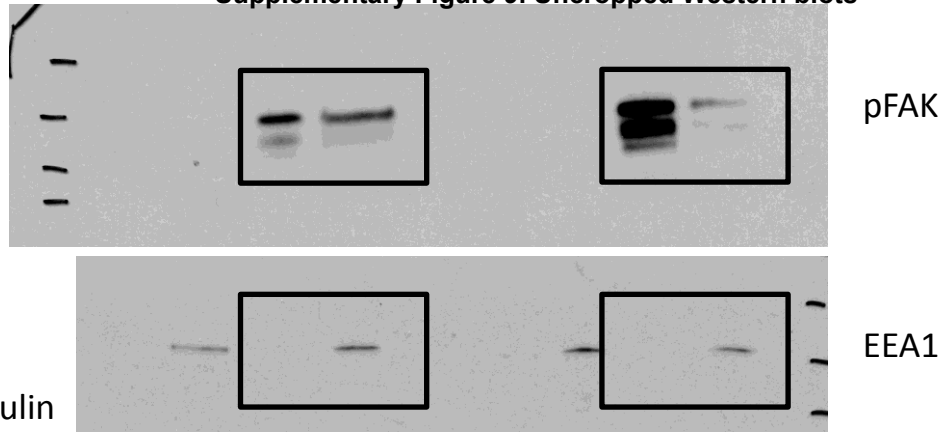


Figure 4d.

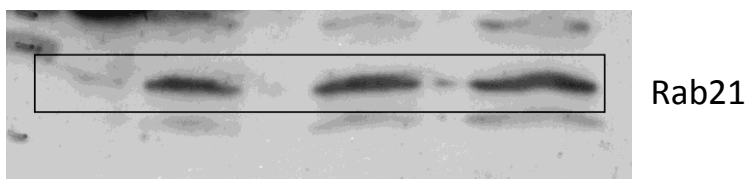
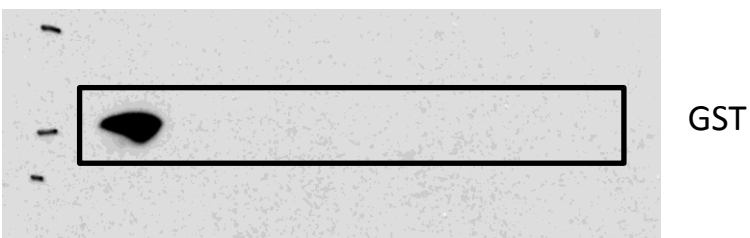
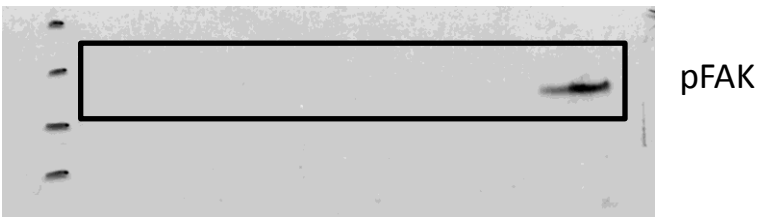
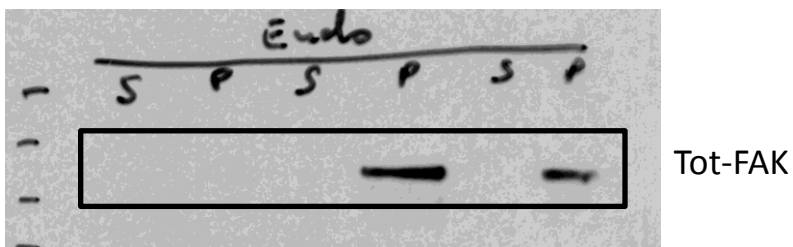


Figure 4e.

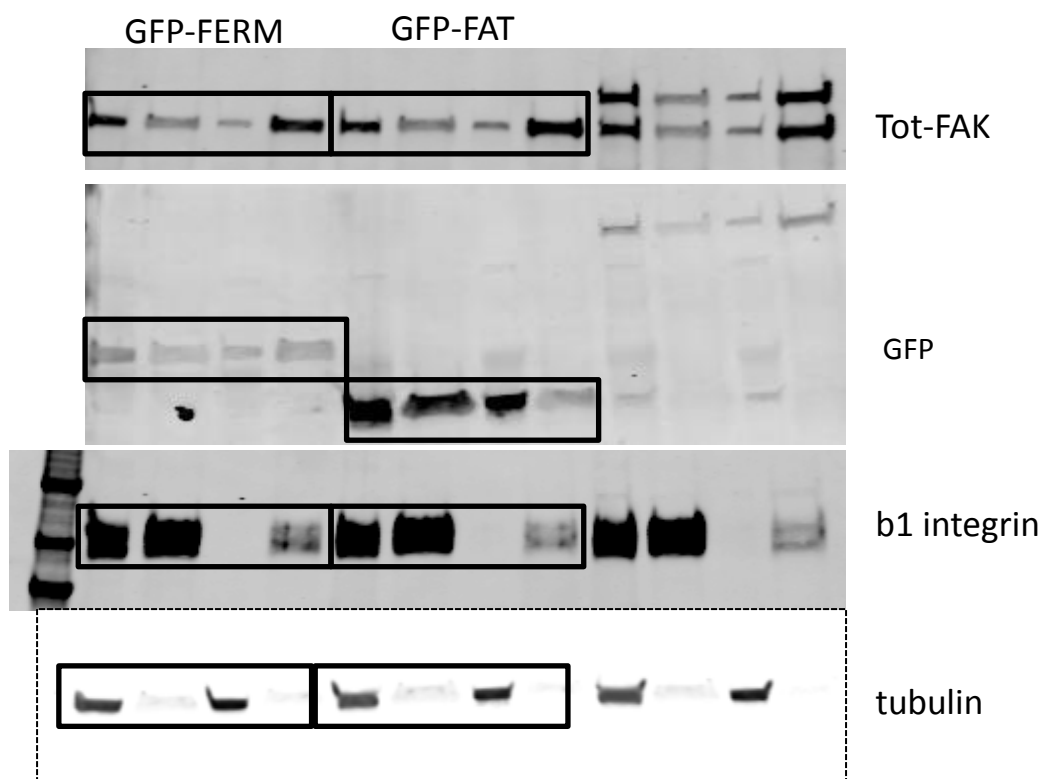


Figure 5a.

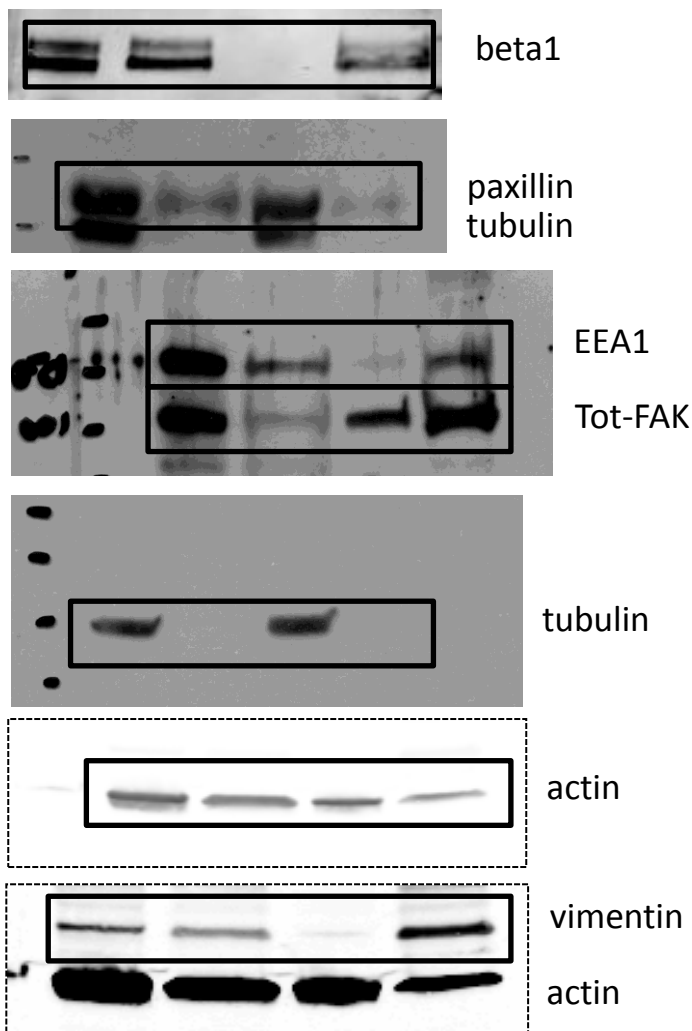


Figure 6a.

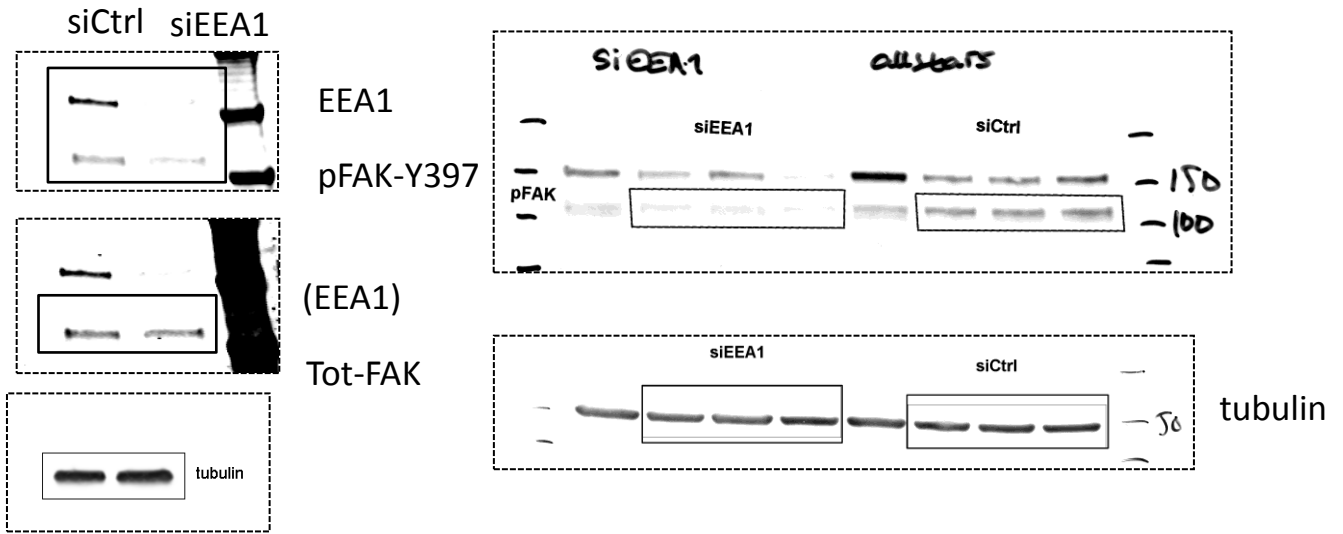


Figure 6b.

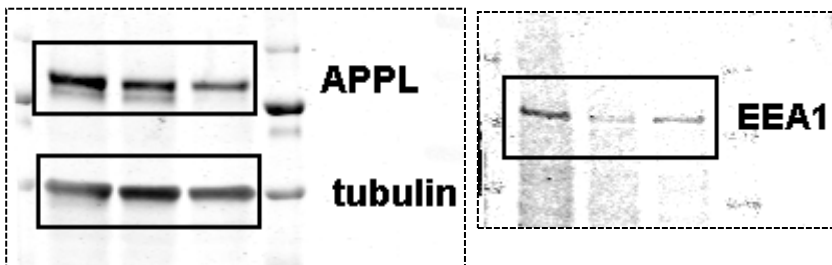


Figure 6c.

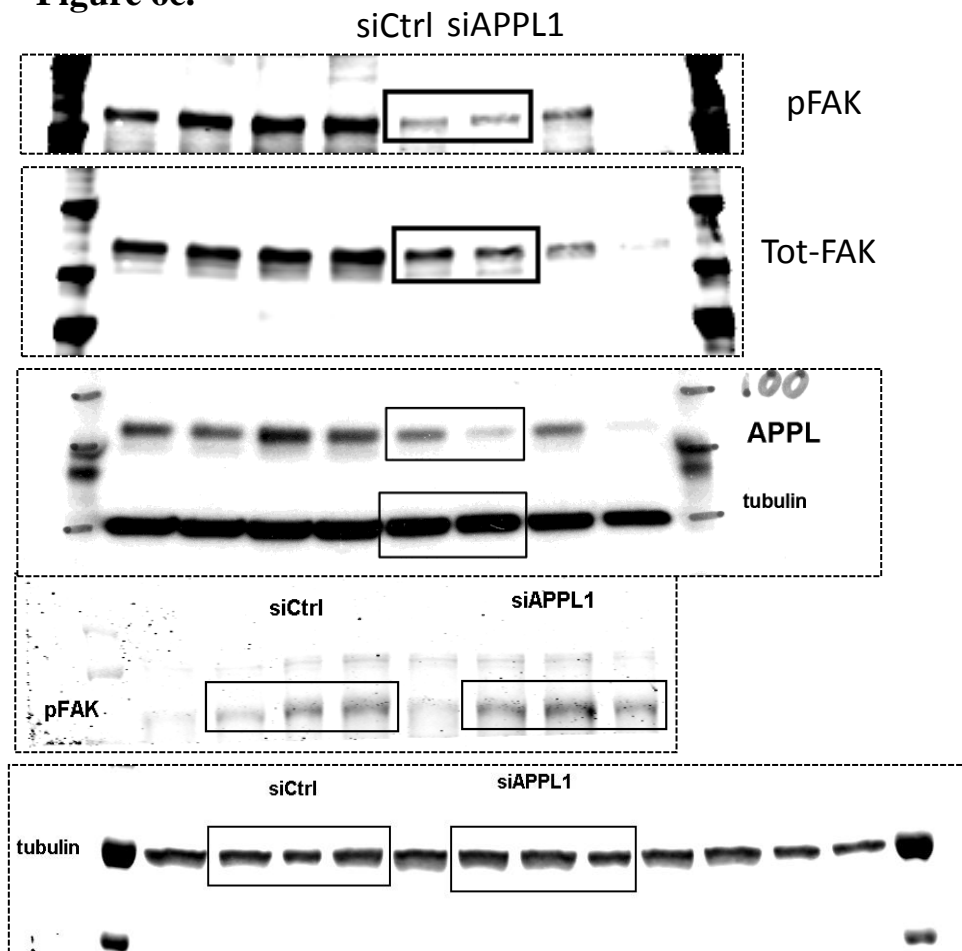


Figure 6d.

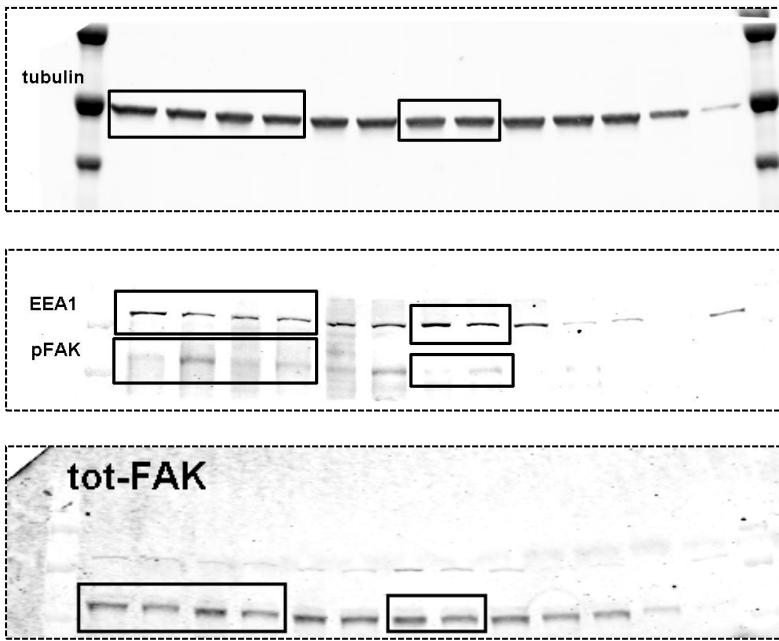


Figure 7b.

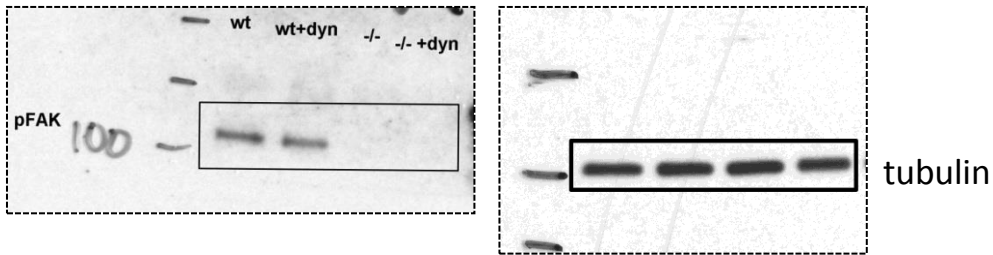


Figure 7f.

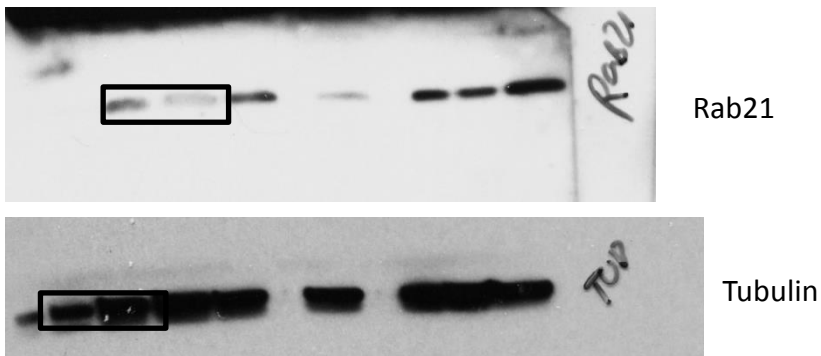
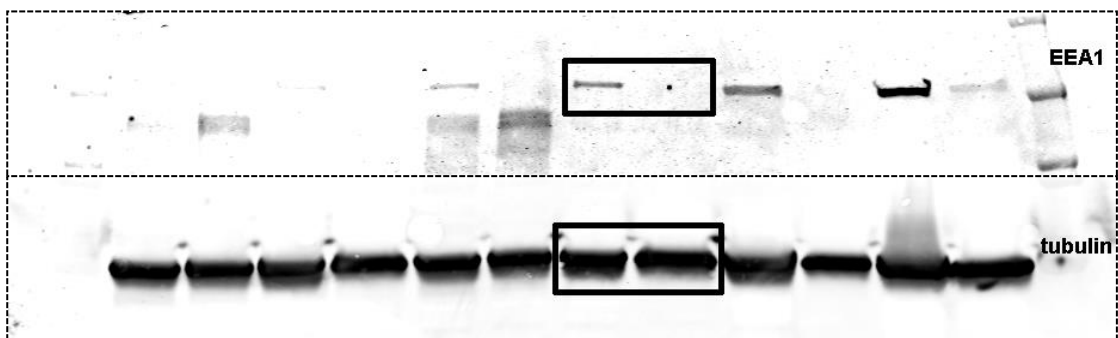
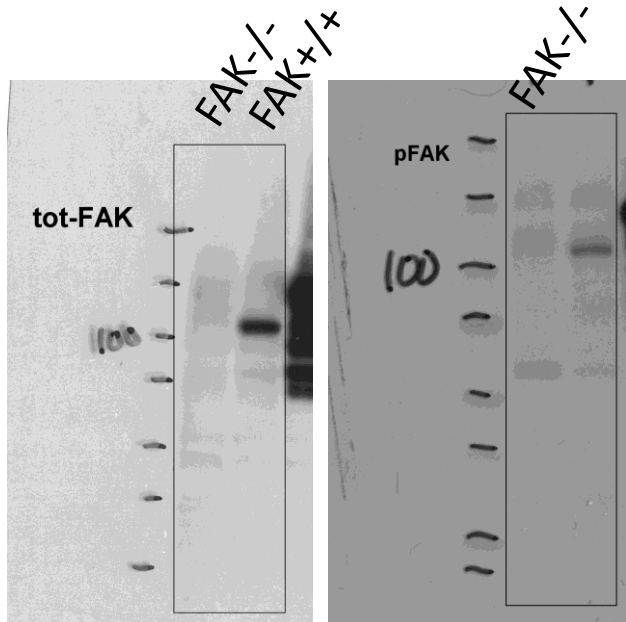


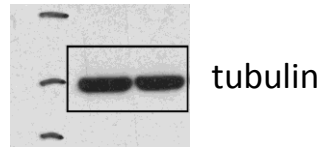
Figure 7g.



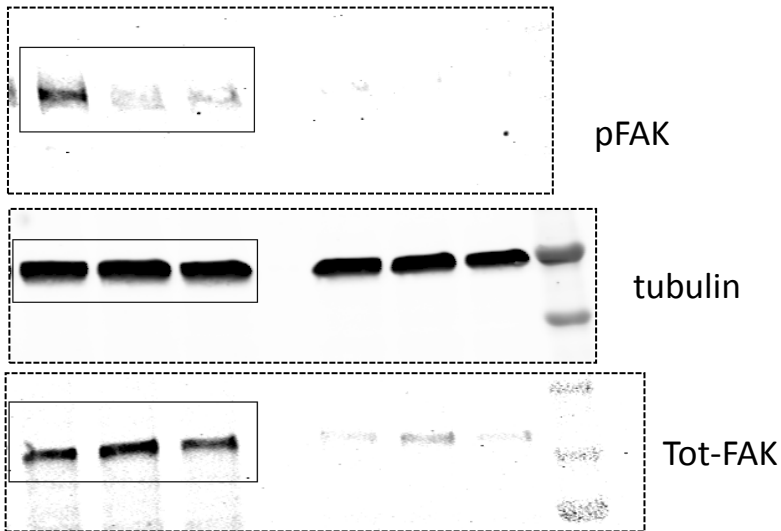
Supplementary Figure 1a.



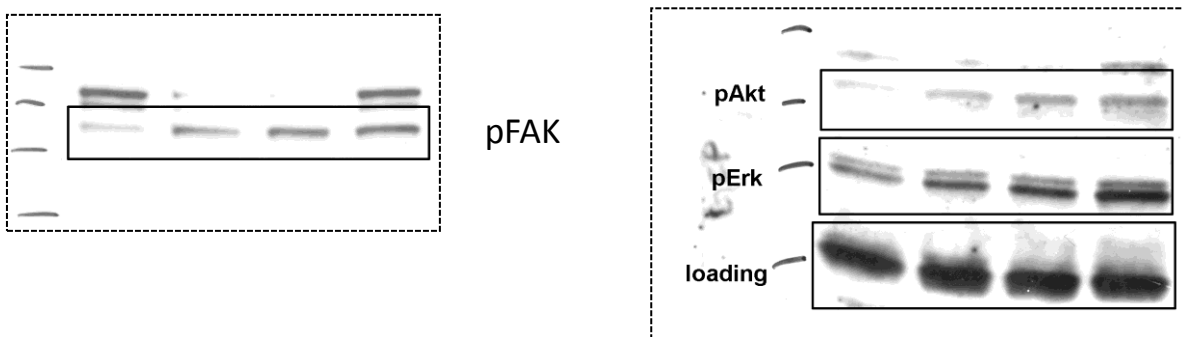
Supplementary Figure 9. Uncropped Western blots



Supplementary Figure 1b.

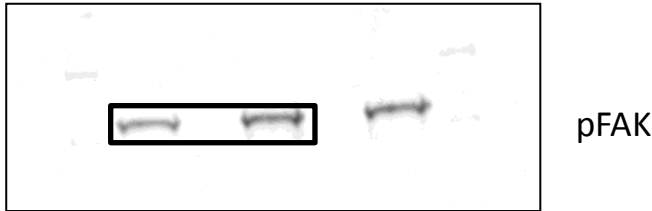
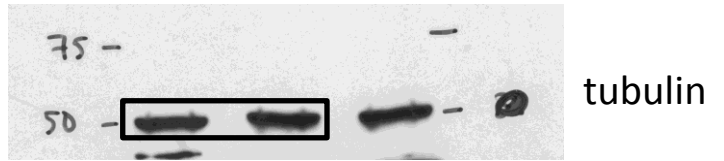
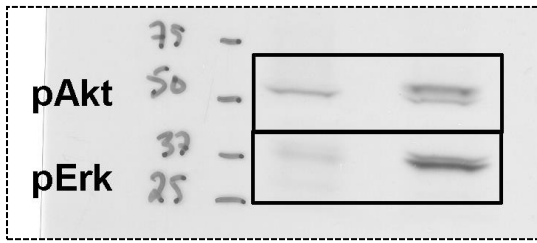


Supplementary Figure 2a.

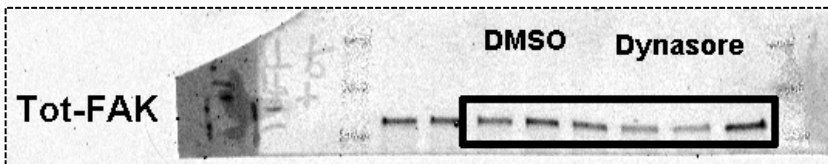
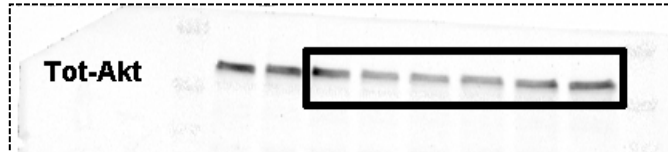
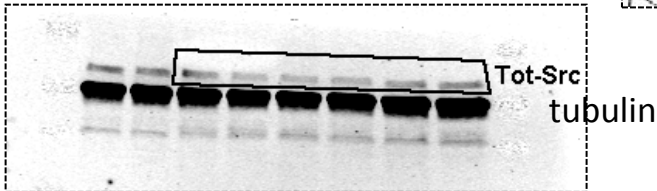
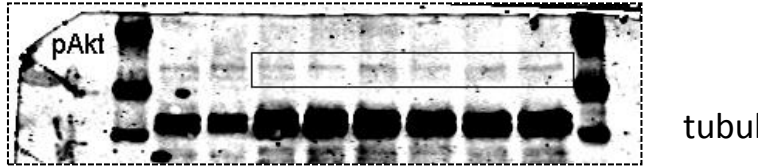
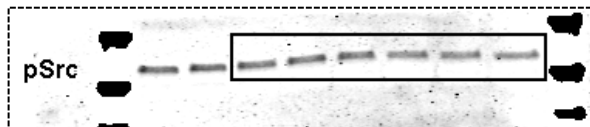
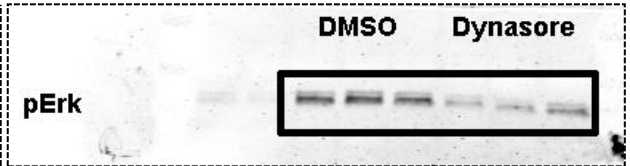
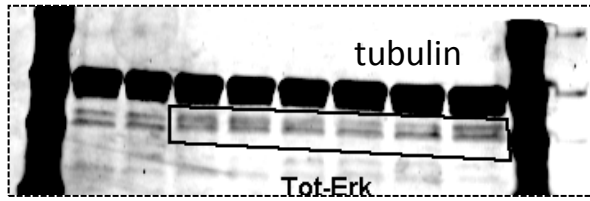
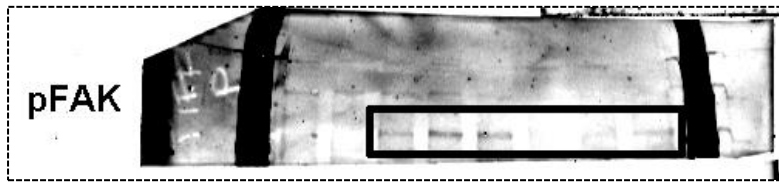


Supplementary Figure 2b.

Supplementary Figure 9. Uncropped Western blots

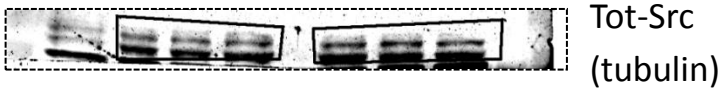
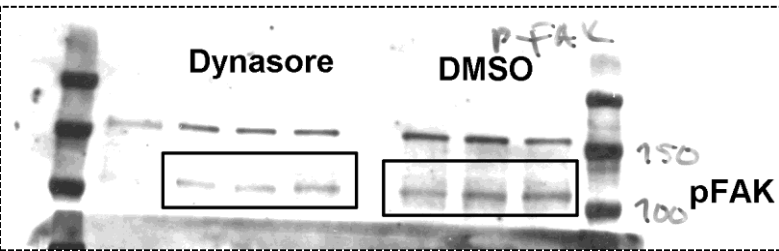
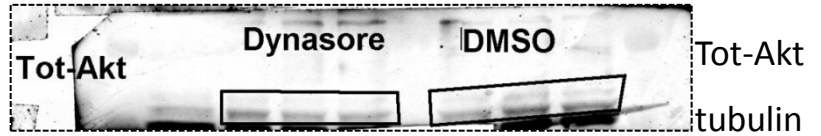
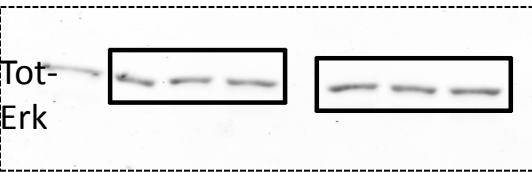
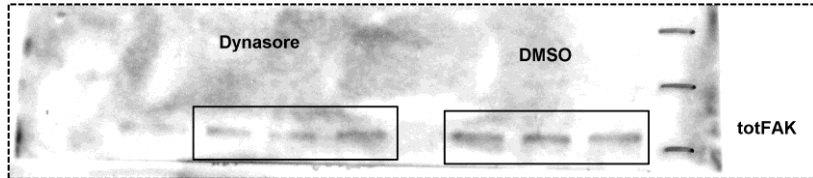
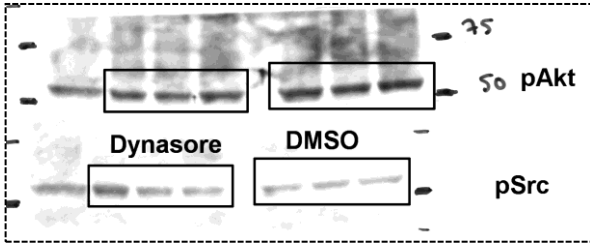
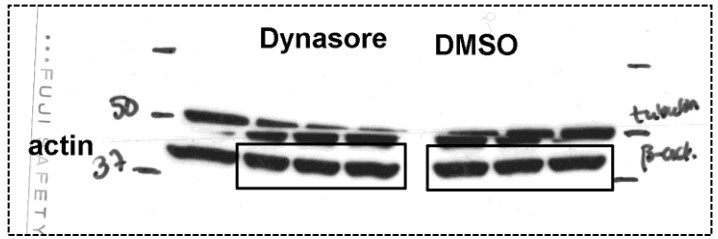
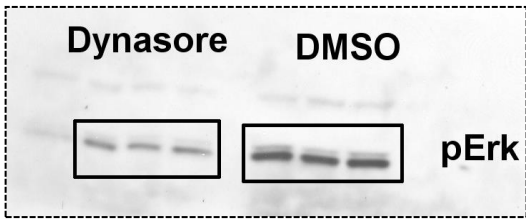


Supplementary Figure 4a.



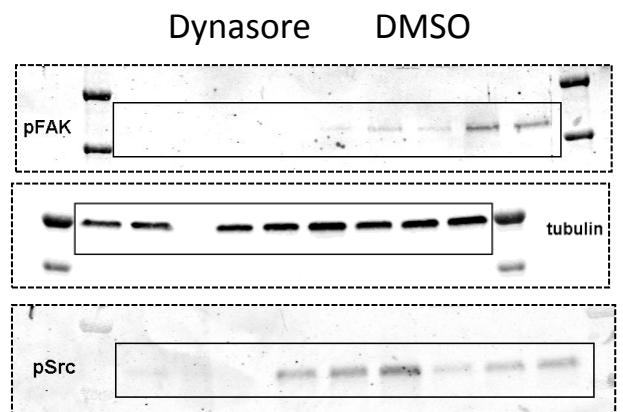
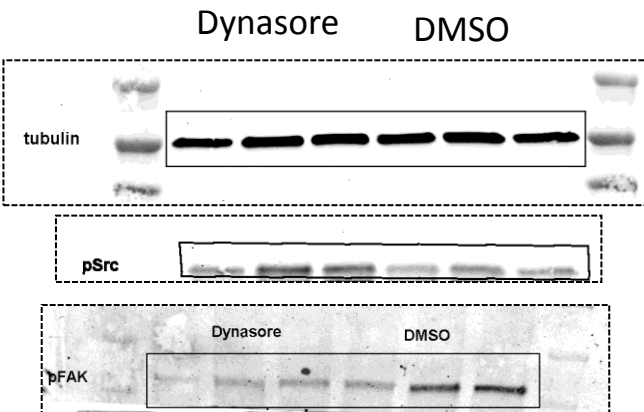
Supplementary Figure 4b.

Supplementary Figure 9. Uncropped Western blots



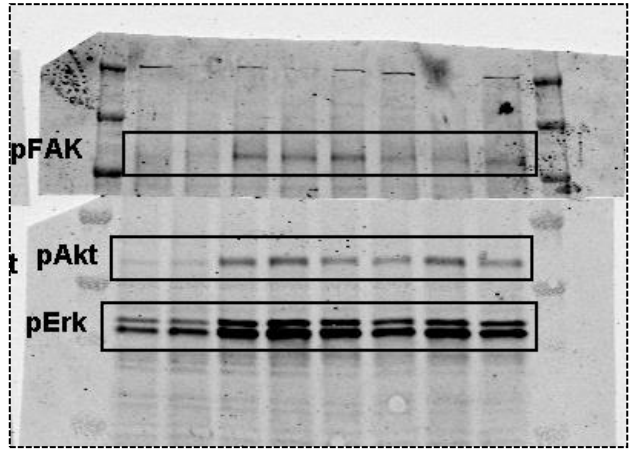
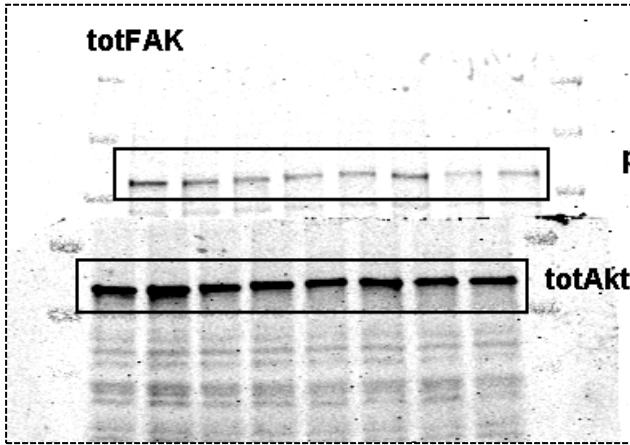
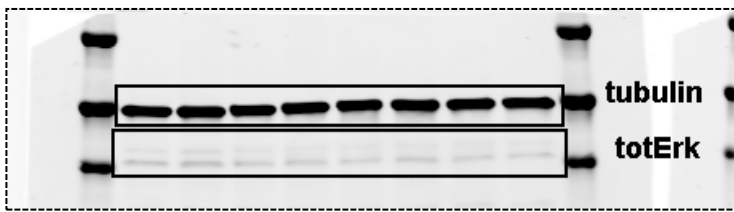
Supplementary Figure 4c.

Supplementary Figure 4d.

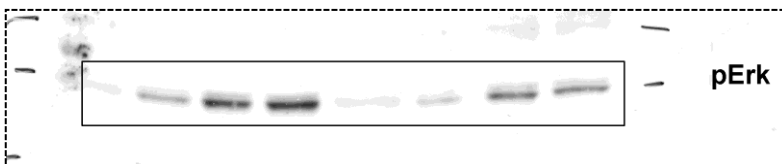
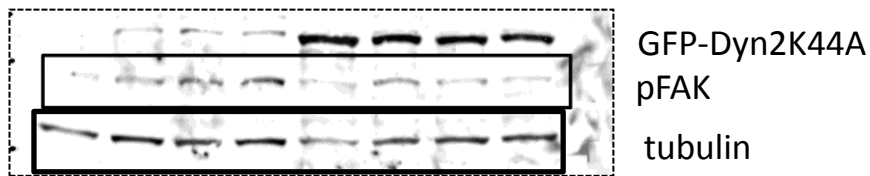
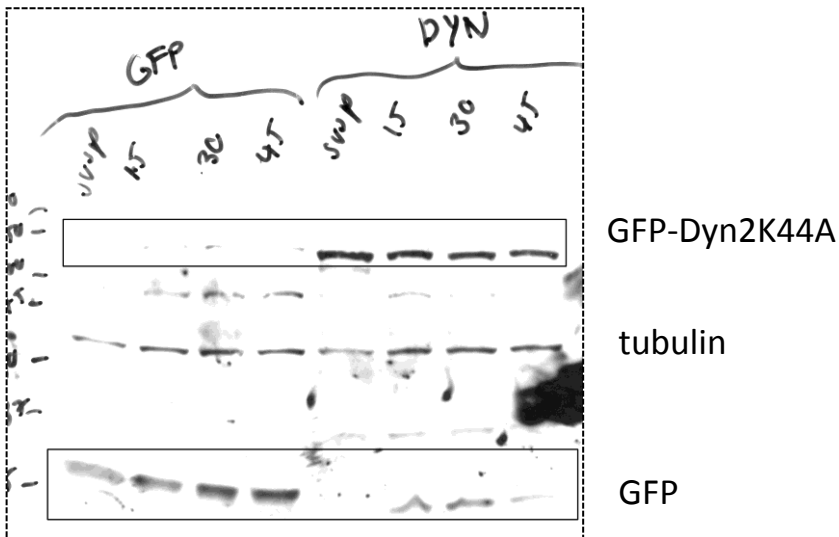


Supplementary Figure 4e.

Supplementary Figure 9. Uncropped Western blots

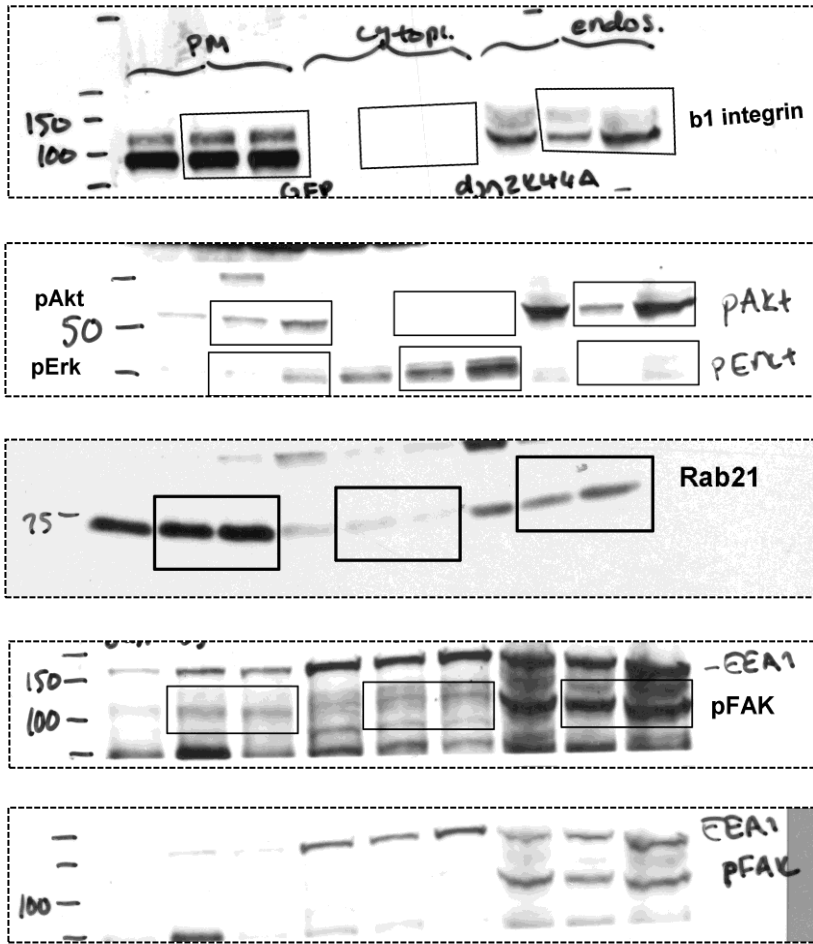


Supplementary Figure 4f.

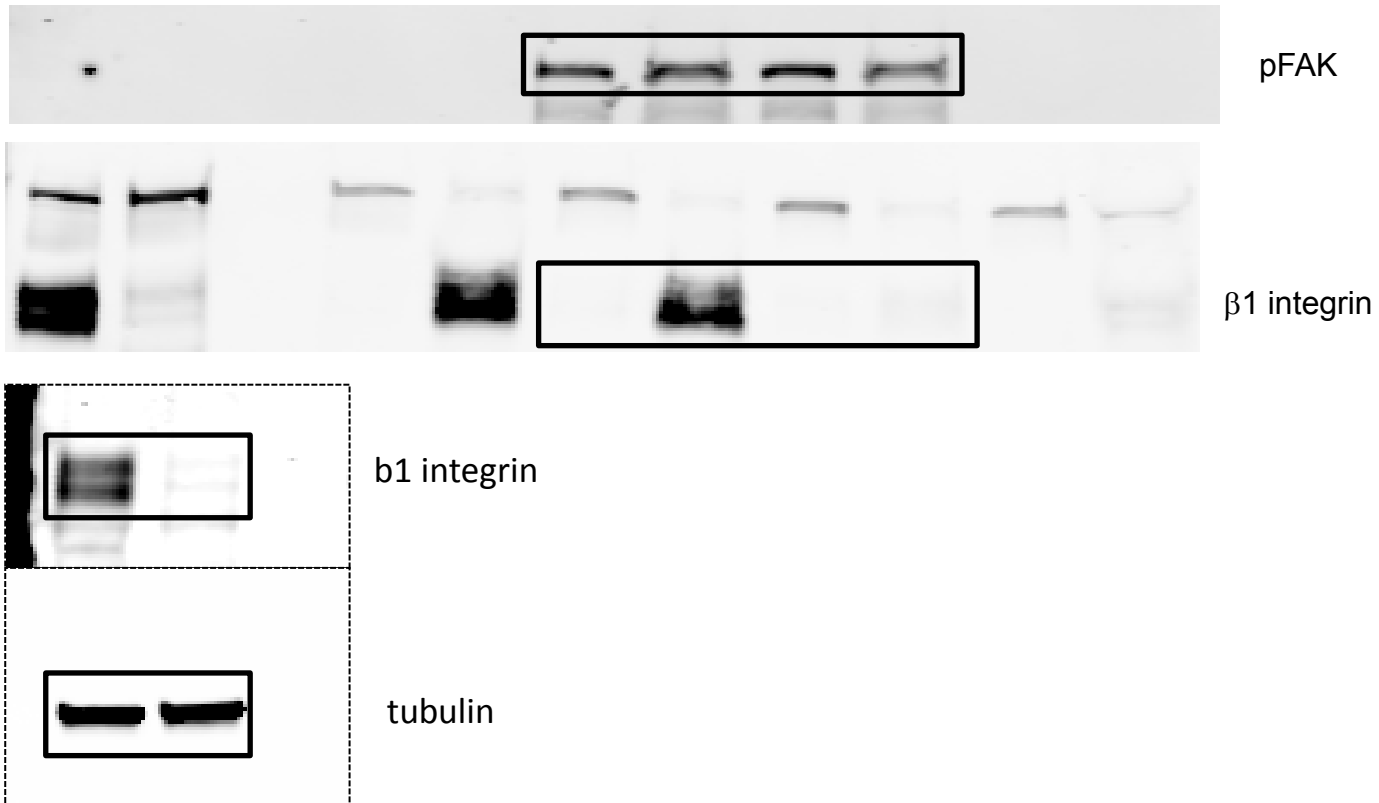


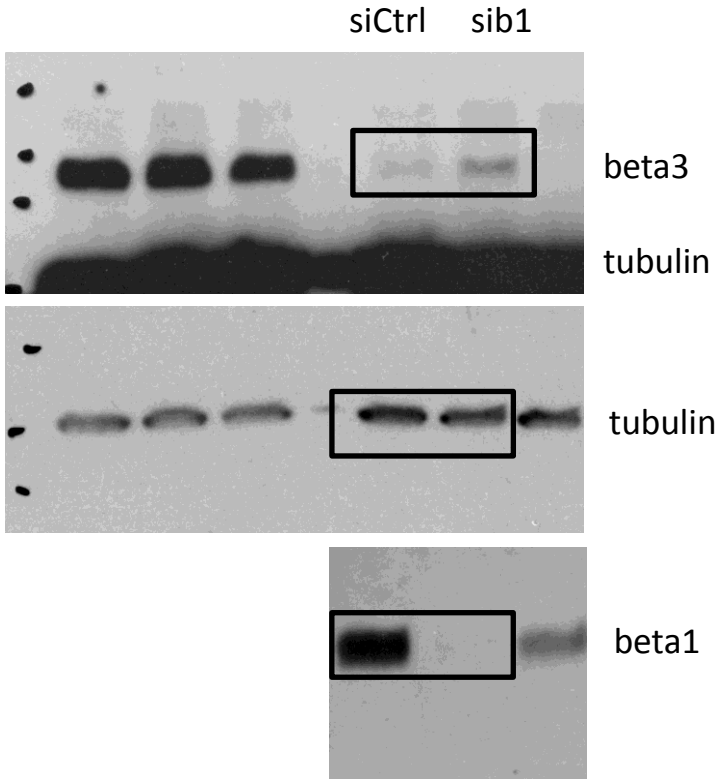
Supplementary Figure 4h.

Supplementary Figure 9. Uncropped Western blots

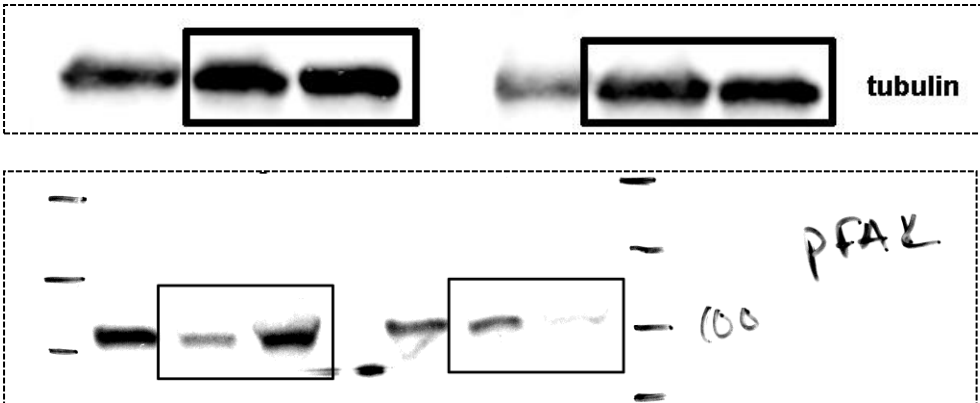


Supplementary Figure 4i.



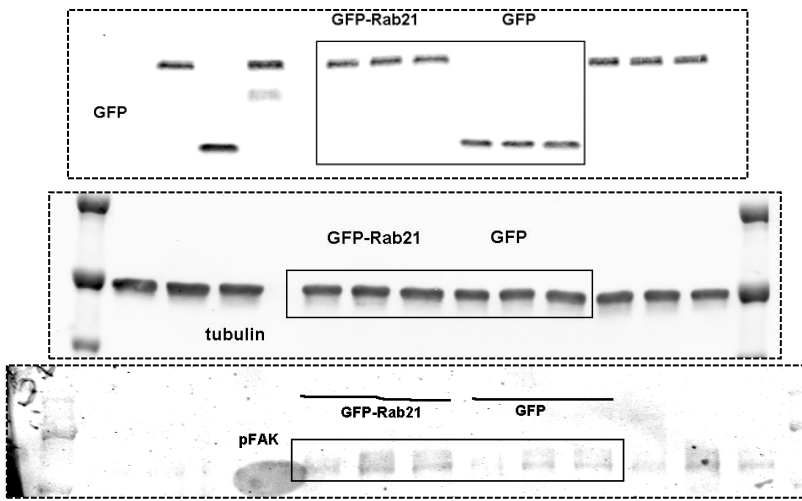


Supplementary Figure 5c.

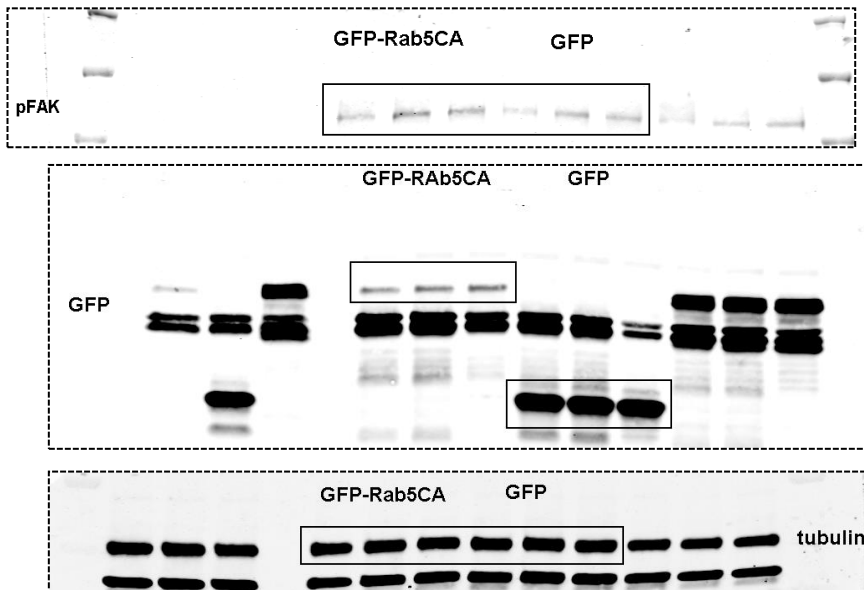


Supplementary Figure 6a.

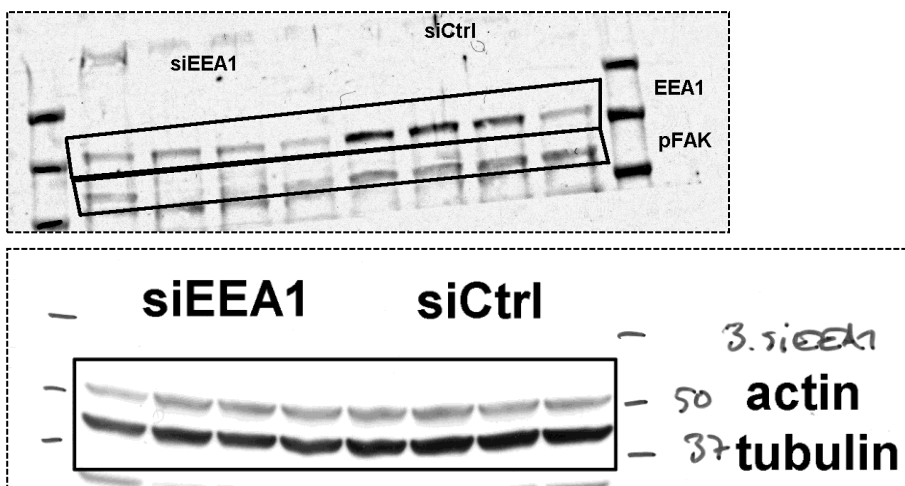
Supplementary Figure 9. Uncropped Western blots



Supplementary Figure 6b.



Supplementary Figure 6d.



Supplementary Figure 9. Uncropped Western blots. Solid line boxes indicate the cropped areas shown in the figures. Dashed lines indicate the outlines of the filter for membranes processed with Odyssey where the background appears white and the signal is strong. In all the uncropped western blot images labelled with more than 1 proteins the filters have been simultaneously or sequentially blotted with the indicated specific antibodies.

Supplementary Table 1. Proteins identified from plasma membrane, endosomal and cytoplasmic fractions. Two biological replicate proteomic analyses (R1 and R2) of proteins isolated from mouse embryonic fibroblast cells were performed. The table shows all proteins identified following database searches using MASCOT and data validation using Scaffold. For each protein, the number of spectra identified from each replicate is shown as well as the normalised spectral counts (normalised to total number of IDs and molecular weight). In addition, column on the left indicate whether each identified proteins is part of the Geiger Adhesome (Zaidel-Bar R et al, 2010) or was previously identified in various MS analyses of adhesion complexes.

Supplementary Table 2. Statistics source data

Supplementary Table 3. List of antibodies and dilutions used in the study